

**DEVELOPMENT OF POLY(β -CYCLODEXTRIN
FUNCTIONALIZED IONIC LIQUID)
CONJUGATED MAGNETIC NANOPARTICLES
AS AN ADSORBENT FOR MICROEXTRACTION
OF POLYCYCLIC AROMATIC
HYDROCARBONS FROM FOOD SAMPLES**

BOON YIH HUI

UNIVERSITI SAINS MALAYSIA

2020

**DEVELOPMENT OF POLY(β -CYCLODEXTRIN
FUNCTIONALIZED IONIC LIQUID)
CONJUGATED MAGNETIC NANOPARTICLES
AS AN ADSORBENT FOR MICROEXTRACTION
OF POLYCYCLIC AROMATIC
HYDROCARBONS FROM FOOD SAMPLES**

by

BOON YIH HUI

**Thesis submitted in fulfilment of the requirements
for the Degree of
Doctor of Philosophy**

April 2020

To My Parents and Family Members
With love

ACKNOWLEDGEMENT

This thesis might have probably never seen light without the support and guidance that I received from many people. I have been lucky enough to spend a few years of my life holding this research under the supervision of my academic advisors, Dr Nadhirah Mohd Zain, Dr Muggundha Raoov, Assc. Prof Dr. Sharifah Mohamad and Prof. Dr. Hasnah Osman. Their invaluable advice, insightful knowledge, patience, and fruitful feedback always motivated me and put me on the right track of my Ph.D. journey. I owe a huge debt of gratitude to them for the successful writing of this thesis.

Sincere thanks to all the laboratory staffs and my research team members from Integrative Medicine Cluster, IPPT for their guidance, helps, and knowledge exchanges throughout my study. In addition, I would also like to give credit to Laboratory FD-L5-4, Department of Chemistry, Universiti Malaya for providing me a conducive environment to conduct my attachment programme. Special appreciation to all the laboratory colleagues and staffs for their assistance and memorable friendships.

Thirdly, I gratefully acknowledge the funding sources that made my Ph.D. study possible. I was honoured to be a scholar funded by Malaysian Pharmaceutical Industries Sdn. Bhd throughout the journey. My work was also supported by the Fundamental Research Grant Scheme (FRGS, 203/CIPPT/6711557), Ministry of Higher Education, Malaysia.

Nobody has been more important in the completion of this project than my family members. Therefore, I would like to thank my grandparents, parents, and siblings for all their loves, prayers, and encouragement throughout this challenging work. Without their unfailing support, I would not have the courage to embark on this journey. Thank you.

TABLE OF CONTENTS

ACKNOWLEDGEMENT	ii
TABLE OF CONTENTS	iii
LIST OF TABLES	viii
LIST OF FIGURES	xi
LIST OF ABBREVIATIONS	xix
LIST OF SYMBOLS	xxiii
ABSTRAK	xxv
ABSTRACT	xxviii
CHAPTER 1 INTRODUCTION	
1.1 General background	1
1.2 Problem Statements	3
1.3 Scope of research	5
1.4 Research objectives	7
1.5 Organization of thesis	8
CHAPTER 2 LITERATURE REVIEW	
2.1 Magnetic nanoparticles (MNPs)	9
2.1.1 Synthesis of MNPs	9
2.1.2 Surface modification of MNPs	10
2.1.3 MNPs in analytical chemistry	11
2.2 Cyclodextrin	16
2.2.1 Properties of cyclodextrin	16
2.2.2 Toxicological considerations	18
2.2.3 Cyclodextrin derivatives	19
2.3 Ionic liquid	21
2.4 Cyclodextrins and ionic liquids-based material in analytical chemistry	22
2.5 Sample preparations for chemical analysis	34

2.5.1	Solid phase extraction (SPE)	34
2.5.2	Microextraction (ME)	39
	2.5.2(a) Magnetic solid phase microextraction (MSPE)	40
	2.5.2(b) Ferrofluid–dispersive liquid phase microextraction (FF-DLPME)	46
2.6	Polycyclic aromatic hydrocarbons (PAHs)	52
	2.6.1 Sources, Properties, and Toxicology	52
	2.6.2 Occurrence of PAHs in food	55
	2.6.3 Occurrence of PAHs in Malaysia	57
2.7	Optimization strategies	59
	2.7.1 Response surface designs	61
2.8	Molecular Modelling	66
	2.8.1 Molecular docking	66
 CHAPTER 3 METHODOLOGY		
3.1	Chemicals, materials and reagents	69
3.2	Characterization Techniques	70
	3.2.1 Thin Layer Chromatography (TLC)	70
	3.2.2 Fourier Transform Infrared (FTIR)	70
	3.2.3 Nuclear Magnetic Resonance (NMR)	70
	3.2.4 Scanning Electron Microscopy (SEM)	71
	3.2.5 Transmission Electron Microscopy (TEM)	71
	3.2.6 Vibrating Sample Magnetometer (VSM)	71
	3.2.7 Nitrogen Adsorption/Desorption Analysis	71
	3.2.8 CHN Elemental Analysis	72
	3.2.9 X-ray powder Diffraction (XRD)	72
	3.2.10 Thermogravimetric Analysis (TGA)	72
	3.2.11 Zeta Potential Analysis	73
	3.2.12 Wettability Analysis	73
	3.2.13 Differential Scanning Calorimetry (DSC)	73

3.2.14	Ultraviolet-visible (UV-Vis) spectrophotometry	74
3.2.15	Gas Chromatographic-Flame Ionization Detector (GC-FID)	74
3.2.16	Gas Chromatographic-Mass Spectrometry (GC-MS)	75
3.3	Preparation of adsorbents	75
3.3.1	Synthesis of poly(β CD-IL)@Fe ₃ O ₄	76
3.3.1(a)	Preparation of <i>p</i> -toluene sulfonic anhydride (Ts ₂ O)	76
3.3.1(b)	Preparation of mono-6-deoxy-6-(<i>p</i> -tosyl)- β -cyclodextrin (β CD-OTs)	76
3.3.1(c)	Preparation of mono-6-deoxy-6-(1-vinylimidazole)- β - cyclodextrin tosylate (β CD-Vinyl-OTs) complex	77
3.3.1(d)	Preparation of poly(β CD-IL)@Fe ₃ O ₄	78
3.3.2	Preparation of ferrofluid	79
3.3.2(a)	Preparation of poly(β CD-IL)@Fe ₃ O ₄ based ferrofluid	79
3.3.2(b)	Stability study	81
3.4	The applications of adsorbents	81
3.4.1	Magnetic micro-solid phase extraction (magnetic μ -SPE)	81
3.4.1(a)	Optimization of magnetic μ -SPE procedures	81
3.4.1(b)	Adopted magnetic μ -SPE procedures	82
3.4.1(c)	Regeneration study	83
3.4.1(d)	Method validation	83
3.4.1(e)	Real samples analysis	86
3.4.1(f)	Comparison study with solid phase extraction	86
3.4.2	Ferrofluid-based dispersive liquid phase microextraction (FF-DLPME)	87
3.4.2(a)	Optimization of FF-DLPME procedures	87
3.4.2(b)	Adopted FF-DLPME procedures	88
3.4.2(c)	Method validation	89
3.4.2(d)	Real samples analysis	90
3.5	Preparation of inclusion complex	91
3.5.1	Preparation and characterization of solid kneaded inclusion complex	91

3.5.2	Preparation of liquid inclusion complex and its spectroscopic determination	92
3.5.3	Molecular modelling	94
3.5.3(a)	Molecular docking	94

CHAPTER 4 RESULTS AND DISCUSSION

4.1	Introduction	95
4.2	Application of magnetic poly(β -cyclodextrin-ionic liquid) nanocomposites for micro-solid phase extraction of selected polycyclic aromatic hydrocarbons from rice prior to GC-FID analysis	96
4.2.1	Synthesis and characterization of poly(β CD-IL)@Fe ₃ O ₄	96
4.2.2	Optimization of poly(β CD-IL)@Fe ₃ O ₄ -based magnetic μ -SPE	115
4.2.3	Regeneration study	128
4.2.4	Analytical performances of poly(β CD-IL)@Fe ₃ O ₄ -based magnetic μ -SPE	129
4.2.5	Real samples analysis	136
4.2.6	Comparison with other reported works	140
4.3	Application of poly(β -cyclodextrin-ionic liquid) based ferrofluid for dispersive liquid phase microextraction of selected polycyclic aromatic hydrocarbons from food and beverage prior to GC-FID analysis	142
4.3.1	Preparation and characterization poly(β CD-IL)@Fe ₃ O ₄ -based ferrofluid	142
4.3.2	Optimization of poly(β CD-IL)@Fe ₃ O ₄ -based FF-DLPME	147
4.3.3	Analytical performances of poly(β CD-IL)@Fe ₃ O ₄ -based FF-DLPME	167
4.3.4	Real sample analysis	174
4.3.5	Comparison with other reported works	180
4.4	Comparison between poly(β CD-IL)@Fe ₃ O ₄ based magnetic μ -SPE and poly(β CD-IL)@Fe ₃ O ₄ based FF-DLPME techniques	182

4.5	Adsorption mechanism of Phenanthrene via inclusion complex study between the native β -CD and ionic liquid modified β -CD	188
4.5.1	Characterization of the solid kneaded inclusion complex	188
4.5.2	Spectroscopic study of the liquid inclusion complex	208
4.5.3	Molecular docking	214

CHAPTER 5 CONCLUSION AND FUTURE DIRECTIONS

5.1	Summary of findings	220
5.2	Recommendations for future work	222

REFERENCES	226
-------------------	-----

APPENDICES

LIST OF PUBLICATIONS

LIST OF PRESENTATIONS

LIST OF TABLES

		Page
Table 2.1	Selected examples of modified MNPs used in MSPE	12
Table 2.2	Selected examples of modified MNPs used in separation science	13
Table 2.3	Selected examples of modified MNPs used in electrochemical sensor	15
Table 2.4	Characteristics of α , β , γ - cyclodextrins	18
Table 2.5	CD-IL modified materials in CE	24
Table 2.6	CD-IL modified materials as chiral stationary phases in HPLC	27
Table 2.7	CD-IL modified materials as enantioselective chiral stationary phases in GC	28
Table 2.8	CD-IL as modifier in CPE	28
Table 2.9	CD-IL modified materials as cross-linked polymer sorbents in SPE	29
Table 2.10	CD-IL modified materials in ME	30
Table 2.11	CD-IL as electrode modifier in electrochemical sensor	31
Table 2.12	CD-IL modified magnetite materials in various applications	32
Table 2.13	Selected applications of SPE technique as sample preparation for PAHs determination in various samples	37
Table 2.14	Selected applications of modified MNPs in MSPE for PAHs determination in various samples	43
Table 2.15	Applications of modified MNPs in FF-DLPME for microextraction of various organic and inorganic pollutants from different samples	50
Table 2.16	16 listed priority PAHs by EPA as major contaminants in food and environmental matrices	53
Table 2.17	New limit fixed by the EC Regulation 835/2011 for benzo[a]pyrene and the sum of PAH4 in foods	56

Table 2.18	PAHs determination in food and beverage samples in Malaysia	58
Table 2.19	Coded factor levels for a Box-Behnken design of a three-variable system with (i.e. 5 centre points)	62
Table 2.20	Selected applications of BBD for the optimization of spectroanalytical methods	64
Table 2.21	Selected applications of BBD for the optimization of chromatographic methods	65
Table 2.22	Selected molecular docking study in determining the preferable orientation between the host and guest molecules	68
Table 4.1	Main IR frequencies with assignment peaks	97
Table 4.2	Content of C, H, and N in Fe ₃ O ₄ , poly(βCD)@Fe ₃ O ₄ and poly(βCD-IL)@Fe ₃ O ₄ nanocomposite	100
Table 4.3	BET analysis of Fe ₃ O ₄ , poly(βCD)@Fe ₃ O ₄ , and poly(βCD-IL)@Fe ₃ O ₄	102
Table 4.4	TGA analysis of Fe ₃ O ₄ , poly(βCD)@Fe ₃ O ₄ and poly(βCD-IL)@Fe ₃ O ₄	109
Table 4.5	DSC analysis of Fe ₃ O ₄ , poly(βCD)@Fe ₃ O ₄ and poly(βCD-IL)@Fe ₃ O ₄	114
Table 4.6	Optimum extraction parameters for the developed magnetic μ-SPE	128
Table 4.7	Analytical figures of merit of the proposed magnetic μ-SPE-GC-FID method	131
Table 4.8	Comparison of the analytical figures of merit between Fe ₃ O ₄ , poly(βCD)@Fe ₃ O ₄ , and SPE (C18)	132
Table 4.9	Relative recoveries for the PAHs extracted from spiked rice samples	133
Table 4.10	Quantitative result of real rice samples analysis	139
Table 4.11	Comparison of the proposed method with counterparts based on the modification of MNPs in MSPE for the extraction of PAHs in various samples	141
Table 4.12	Main IR frequencies with assignment peaks	143
Table 4.13	The experimental results for Box-Behnken design with the independent variables	156

Table 4.14	Analysis of variance (ANOVA) and validation of response surface model	158
Table 4.15	Optimum parameters for the developed FF-DLPME	167
Table 4.16	Analytical figures of merit of the proposed FF-DLPME-GC-FID method in water, rice, and tea matrices	169
Table 4.17	Relative recoveries for the PAHs extracted from various spiked food and beverage samples	172
Table 4.18	PAHs determined in various food samples by the proposed FF-DLPME	176
Table 4.19	Analytical figures of merit of the proposed FF-DLPME-GC-FID method in the urine of non-smoker	179
Table 4.20	Relative recoveries for the PAHs extracted from spiked urine samples	179
Table 4.21	Comparison of the proposed method with counterparts based on the modification of MNPs for the extraction of PAHs in various samples	181
Table 4.22	Comparison of the analytical performance for the developed magnetic μ -SPE and FF-DLPME techniques	184
Table 4.23	IR peak assignments of Phe, β CD and their solid inclusion complex	192
Table 4.24	IR peak assignments of Phe, β CD-IL and their solid inclusion complex	193
Table 4.25	^1H chemical shifts values corresponding to the β CD, Phe and inclusion complex of β CD and Phe	200
Table 4.26	^1H chemical shifts values corresponding to the β CD-IL, Phe and inclusion complex of β CD-IL and Phe	202
Table 4.27	Summary of the spectroscopic determination	214
Table 4.28	Scores of the top 10 docked models of Phe: β CD inclusion complex computed using Patch Dock server	215
Table 4.29	Scores of the top 10 docked models of Phe: β CD-IL inclusion complex computed using Patch Dock server	216

LIST OF FIGURES

		Page
Figure 2.1	Structure of the core, shell of various composition, and the coating with different functional groups	11
Figure 2.2	Chemical structure of α -CDs, β -CDs and γ -CDs	17
Figure 2.3	α -1,4 glucopyranose units linkages and the numbering system in a CD molecule	17
Figure 2.4	Hydrophobic cavity and hydrophilic exterior of a CD molecule	17
Figure 2.5	Schematic illustration of the association of free host (cyclodextrin) and guest molecules to form inclusion complex	18
Figure 2.6	Tosylation of β -CD to form C6-tosyl- β -CD	20
Figure 2.7	Common structures of cations and anions	22
Figure 2.8	Formation of CD-IL complex through (a) functionalization process (b) loading process	23
Figure 2.9	Three components of SPE: disks, cartridges, and syringe barrel	35
Figure 2.10	The presentation of MSPE procedures	41
Figure 2.11	Schematic illustration of possible distribution of nanoparticles in the ferrofluids	47
Figure 2.12	Flow of the optimization strategies	60
Figure 2.13	Schematic illustration of a Box-Behnken design with three factors, A, B and C and one centre point	61
Figure 2.14	Outline of the molecular docking process	66
Figure 3.1	Reaction pathway for the preparation of <i>p</i> -toluene sulfonic anhydride	76
Figure 3.2	Synthesis pathway of poly(β CD-IL)@Fe ₃ O ₄	79
Figure 3.3	Schematic diagram for the preparation of ferrofluid	80
Figure 3.4	The digital photograph image of ferrofluid as described	80

Figure 3.5	Schematic view of magnetic μ -SPE experimental setup	82
Figure 3.6	Schematic illustration of the FF-DLPME procedure	88
Figure 3.7	Schematic illustration of the kneading method for inclusion complex formation	92
Figure 4.1	FTIR spectra of (a) Fe_3O_4 , (b) $\text{poly}(\beta\text{CD})@\text{Fe}_3\text{O}_4$, and (c) $\text{poly}(\beta\text{CD-IL})@\text{Fe}_3\text{O}_4$	97
Figure 4.2	Water contact angle of (a) Fe_3O_4 , (b) $\text{poly}(\beta\text{CD})@\text{Fe}_3\text{O}_4$, and (c) $\text{poly}(\beta\text{CD-IL})@\text{Fe}_3\text{O}_4$	98
Figure 4.3	VSM spectra (a) Fe_3O_4 , (b) $\text{poly}(\beta\text{CD})@\text{Fe}_3\text{O}_4$, and (c) $\text{poly}(\beta\text{CD-IL})@\text{Fe}_3\text{O}_4$	100
Figure 4.4	N_2 adsorption-desorption isotherms of (a) Fe_3O_4 , (b) $\text{poly}(\beta\text{CD})@\text{Fe}_3\text{O}_4$, and (c) $\text{poly}(\beta\text{CD-IL})@\text{Fe}_3\text{O}_4$	103
Figure 4.5	XRD spectra of (a) Fe_3O_4 , (b) $\text{poly}(\beta\text{CD})@\text{Fe}_3\text{O}_4$, (c) $\text{poly}(\beta\text{CD-IL})@\text{Fe}_3\text{O}_4$	105
Figure 4.6	The zeta potential of (a) Fe_3O_4 , (b) $\text{poly}(\beta\text{CD})@\text{Fe}_3\text{O}_4$ and (c) $\text{poly}(\beta\text{CD-IL})@\text{Fe}_3\text{O}_4$	106
Figure 4.7	TGA and DTG (inset) analysis of (a) Fe_3O_4 , (b) $\text{poly}(\beta\text{CD})@\text{Fe}_3\text{O}_4$ and (c) $\text{poly}(\beta\text{CD-IL})@\text{Fe}_3\text{O}_4$	108
Figure 4.8	SEM images of (a) Fe_3O_4 , (b) $\text{poly}(\beta\text{CD})@\text{Fe}_3\text{O}_4$, and (c) $\text{poly}(\beta\text{CD-IL})@\text{Fe}_3\text{O}_4$	111
Figure 4.9	TEM images and diameter distributions of (a) Fe_3O_4 , (b) $\text{poly}(\beta\text{CD})@\text{Fe}_3\text{O}_4$, and (c) $\text{poly}(\beta\text{CD-IL})@\text{Fe}_3\text{O}_4$	112
Figure 4.10	DSC curves of (a) Fe_3O_4 , (b) $\text{poly}(\beta\text{CD})@\text{Fe}_3\text{O}_4$ and (c) $\text{poly}(\beta\text{CD-IL})@\text{Fe}_3\text{O}_4$	114
Figure 4.11	Comparison of extraction efficiencies of PAHs with different adsorbents. (Extraction conditions: extraction sorbent amount, 20 mg; eluent volume, 1.5 mL of ACN; extraction time, 30 min; desorption time, 30 min, sample solution, 20 mL)	116
Figure 4.12	The proposed adsorption mechanism of targeted PAHs towards $\text{poly}(\beta\text{CD-IL})@\text{Fe}_3\text{O}_4$	116

Figure 4.13	The effect of amount of sorbent on the extraction efficiency of PAHs. (Extraction conditions: eluent volume, 1.5 mL of ACN; extraction time, 30 min; desorption time, 30 min, sample solution, 20 mL)	118
Figure 4.14	The effect of extraction time on the extraction efficiency of PAHs. (Extraction conditions: extraction sorbent amount, 20 mg; eluent volume, 1.5 mL of ACN; desorption time, 30 min, sample solution, 20 mL)	119
Figure 4.15	The effect of ionic strength on the extraction efficiency of PAHs. (Extraction conditions: extraction sorbent amount, 20 mg; extraction time, 30 min; eluent volume, 1.5 mL of ACN; desorption time, 30 min, sample solution, 20 mL)	120
Figure 4.16	The effect of desorption solvent on the extraction efficiency of PAHs. (Extraction conditions: extraction sorbent amount, 20 mg; extraction time, 30 min; ionic strength, 3% (w/v) of NaCl; eluent volume, 1.5 mL; desorption time, 30 min, sample solution, 20 mL)	122
Figure 4.17	The effect of desorption volume on the extraction efficiency of PAHs. (Extraction conditions: extraction sorbent amount, 20 mg; extraction time, 30 min; ionic strength, 3% (w/v) of NaCl; eluent, ACN; desorption time, 30 min, sample solution, 20 mL)	123
Figure 4.18	The effect of desorption time on the extraction efficiency of PAHs. (Extraction conditions: extraction sorbent amount, 20 mg; extraction time, 30 min; ionic strength, 3% (w/v) of NaCl; eluent volume, 200 μ L of ACN; sample solution, 20 mL)	124
Figure 4.19	The effect of pH on the extraction efficiency of PAHs. (Extraction conditions: extraction sorbent amount, 20 mg; extraction time, 30 min; ionic strength, 3% (w/v) of NaCl; eluent volume, 200 μ L of ACN; desorption time, 15 min, sample solution, 20 mL)	125
Figure 4.20	The effect of organic modifier on the extraction efficiency of PAHs. (Extraction conditions: extraction sorbent amount, 20 mg; extraction time, 30 min; ionic strength, 3% (w/v) of NaCl without pH adjustment; eluent volume, 200 μ L of ACN; desorption time, 15 min, sample solution, 20 mL)	126
Figure 4.21	The effect of sample volume on the extraction efficiency of PAHs. (Extraction conditions: extraction sorbent amount, 20 mg; extraction time, 30 min; ionic strength, 3% (w/v) of NaCl without pH adjustment; eluent volume, 200 μ L of ACN without organic modifier, desorption time, 15 min)	127

Figure 4.22	Reusability cycle of poly(β CD-IL)@Fe ₃ O ₄ as magnetic μ -SPE nanosorbents	129
Figure 4.23	Magnetic μ -SPE-GC-FID chromatograms of rice samples extract using the optimum procedure. (a) blank rice sample; (b) blank spiked rice sample (10 μ g kg ⁻¹), and (c) blank spiked rice sample (100 μ g kg ⁻¹) obtained after extraction	134
Figure 4.24	Magnetic μ -SPE-GC-FID chromatograms of different real rice samples extract using the optimum procedure with Phenanthrene was detected in all the tested samples	135
Figure 4.25	Toxic Equivalent Factor (TEF) for each of the tested rice groups	138
Figure 4.26	(a) GC-MS chromatogram of white rice S10, (b, c) mass spectra of non-spiked rice S10; (d, e) reference mass spectra from library	138
Figure 4.27	FT-IR spectra of (a) unmodified poly(β CD-IL)@Fe ₃ O ₄ and (b) modified poly(β CD-IL)@Fe ₃ O ₄	143
Figure 4.28	SEM micrographs of (a) unmodified poly(β CD-IL)@Fe ₃ O ₄ under magnification of 25.0 k and (b) modified poly(β CD-IL)@Fe ₃ O ₄ under magnification of 10.0 k	144
Figure 4.29	FTIR spectra of the prepared ferrofluid after (a) first and (b) fifth week of formation and storage at room temperature	145
Figure 4.30	SEM micrographs of the prepared ferrofluid after (a) first and (b) fifth week of formation and storage at room temperature	146
Figure 4.31	Comparison of extraction efficiencies of PAHs using (a) poly(β CD-IL)@Fe ₃ O ₄ and (b) poly(β CD-IL)@Fe ₃ O ₄ based ferrofluid. (Extraction conditions: extraction sorbent amount, 10 mg; ferrofluid formation time, 10 min; volume and type of SUPRAS, 100 μ L of 1-octanol; extraction time, 5 min; eluent volume, 0.5 mL of ACN; desorption time, 3 min, sample solution, 15 mL)	148
Figure 4.32	(A) Effect of type of carrier liquid on extraction efficiency of PAHs based on single factor experiments. (Extraction conditions: ferrofluid formation time, 10 min; extraction sorbent amount, 10 mg; volume of SUPRAS, 100 μ L; extraction time, 5 min; eluent volume, 0.5 mL of ACN; desorption time, 3 min, sample solution, 15 mL). (B)(i) FFs that formed in ideal and (ii) highly hydrophobic environment	150

Figure 4.33	Effect of amount of sorbent used in preparing the ferrofluid on the extraction efficiency of PAHs based on single factor experiments. (Extraction conditions: ferrofluid formation time, 10 min; volume and type of SUPRAS, 100 μ L of 1-octanol; extraction time, 5 min; eluent volume, 0.5 mL of ACN; desorption time, 3 min, sample solution, 15 mL)	151
Figure 4.34	Effect of ionic strength on the extraction efficiency of PAHs based on single factor experiments. (Extraction conditions: ferrofluid formation time, 10 min; extraction sorbent amount, 10 mg; volume and type of SUPRAS, 100 μ L of 1-octanol; extraction time, 5 min; eluent volume, 0.5 mL of ACN; desorption time, 3 min, sample solution, 15 mL)	152
Figure 4.35	Effect of ferrofluid formation time on the extraction efficiency of PAHs based on single factor experiments. (Extraction conditions: extraction sorbent amount, 10 mg; volume and type of SUPRAS, 100 μ L of 1-octanol; extraction time, 5 min; eluent volume, 0.5 mL of ACN; desorption time, 3 min, sample solution, 15 mL with 2% NaCl)	153
Figure 4.36	Effect of volume of SUPRAS on the extraction efficiency of PAHs based on single factor experiments. (Extraction conditions: ferrofluid formation time, 10 min; extraction sorbent amount, 10 mg; type of SUPRAS, 1-octanol; extraction time, 5 min; eluent volume, 0.5 mL of ACN; desorption time, 3 min, sample solution, 15 mL with 2% NaCl)	154
Figure 4.37	Effect of extraction time on the extraction efficiency of PAHs based on single factor experiments. (Extraction conditions: ferrofluid formation time, 10 min; extraction sorbent amount, 10 mg; volume and type of SUPRAS, 50 μ L of 1-octanol; eluent volume, 0.5 mL of ACN; desorption time, 3 min, sample solution, 15 mL with 2% NaCl)	155
Figure 4.38	Residual plot of the predicted extraction response according to the regression	158
Figure 4.39	Response surface from the Box-Behnken design for the total peak area of the extracted PAHs	161
Figure 4.40	Plot of predicted versus observed values for total peak area of PAHs	162

Figure 4.41	Effect of type of desorption solvent on the extraction efficiency of PAHs. (Extraction conditions: ferrofluid formation time, 5 min; extraction sorbent amount, 10 mg; volume and type of SUPRAS, 90 μL of 1-octanol; extraction time, 5 min; eluent volume, 0.5 mL; desorption time, 3 min, sample solution, 15 mL with 2% NaCl)	163
Figure 4.42	Effect of desorption solvent volume on the extraction efficiency of PAHs. (Extraction conditions: ferrofluid formation time, 5 min; extraction sorbent amount, 10 mg; volume and type of SUPRAS, 90 μL of 1-octanol; extraction time, 5 min; type of eluent, DCM; desorption time, 3 min, sample solution, 15 mL with 2% NaCl)	164
Figure 4.43	Effect of desorption time on the extraction efficiency of PAHs. (Extraction conditions: ferrofluid formation time, 5 min; extraction sorbent amount, 10 mg; volume and type of SUPRAS, 90 μL of 1-octanol; extraction time, 5 min; volume and type of eluent, 300 μL of DCM; sample solution, 15 mL with 2% NaCl)	165
Figure 4.44	Effect of sample volume on the extraction efficiency of PAHs. (Extraction conditions: ferrofluid formation time, 5 min; extraction sorbent amount, 10 mg; volume and type of SUPRAS, 90 μL of 1-octanol; extraction time, 5 min; volume and type of eluent, 300 μL of DCM; desorption time, 1 min; sample solution, 2% NaCl)	166
Figure 4.45	Chromatogram of (a) green tea sample spiked with 30 ng mL^{-1} of PAHs and (b) blank green tea sample after FF-DLPME. Peak identification: 1, Acenaphthalene; 2, Fluorene; 3, Phenanthrene; 4, Fluoranthene; 5, Pyrene; 6, Benzo(a) anthracene; 7, Benzo(a) Pyrene	173
Figure 4.46	Chromatogram of (a) rice sample spiked with 50 $\mu\text{g kg}^{-1}$ of PAHs; (b) blank rice sample and (c) blank smoky food seasoning sample after FF-DLPME. Peak identification: 1, Acenaphthalene; 2, Fluorene; 3, Phenanthrene; 4, Fluoranthene; 5, Pyrene; 6, Benzo(a) anthracene; 7, Benzo(a) Pyrene	173
Figure 4.47	Chromatogram of (a) blank urine sample spiked with 30 ng mL^{-1} of PAHs and (b) blank urine sample of smoker after FF-DLPME. Peak identification: 1, Acenaphthalene; 2, Fluorene; 3, Phenanthrene; 4, Fluoranthene; 5, Pyrene; 6, Benzo(a) anthracene; 7, Benzo(a) Pyrene	180

Figure 4.48	Comparison of the analytical signal (peak area) obtained from GC-FID system using spiked rice at level 300 $\mu\text{g kg}^{-1}$ under optimized FF-DLPME and magnetic $\mu\text{-SPE}$ conditions	186
Figure 4.49	Comparison of the GC-FID chromatograms obtained after (a) FF-DLPME and (b) MSPE from rice at spiked level 300 $\mu\text{g kg}^{-1}$ under optimized conditions. Peak identification: 1, Acenaphthalene; 2, Fluorene; 3, Phenanthrene; 4, Fluoranthene; 5, Pyrene; 6, Benzo(a) anthracene; 7, Benzo(a) Pyrene	187
Figure 4.50	FTIR spectra of (a) βCD , (b) Phe and (c) solid inclusion complex	191
Figure 4.51	FTIR spectra of (a) $\beta\text{CD-IL}$, (b) Phe and (c) solid inclusion complex	191
Figure 4.52	(a) TGA and (b) DTG thermogram of (A) βCD ; (B) Phe; (C) inclusion complex of $\beta\text{CD-Phe}$; (D) $\beta\text{CD-IL}$; and (E) inclusion complex of $\beta\text{CD-IL-Phe}$	195
Figure 4.53	The DSC curves of (a) βCD ; (b) Phe; and (c) inclusion complex of βCD with Phe	197
Figure 4.54	The DSC curves of (a) $\beta\text{CD-IL}$; (b) Phe; and (c) inclusion complex of $\beta\text{CD-IL}$ with Phe	197
Figure 4.55	^1H NMR spectra of (a) βCD ; (b) Phe; and (c) inclusion complex of βCD and Phe in DMSO-d_6	201
Figure 4.56	^1H NMR spectra of (a) $\beta\text{CD-IL}$; (b) Phe; and (c) inclusion complex of $\beta\text{CD-IL}$ and Phe in DMSO-d_6	203
Figure 4.57	The two-dimensional NOESY spectrum of $\beta\text{CD-Phe}$ inclusion complex in DMSO-d_6	205
Figure 4.58	The two-dimensional NOESY spectrum of $\beta\text{CD-IL-Phe}$ inclusion complex in DMSO-d_6	206
Figure 4.59	The proposed structures of inclusion complex between βCD and Phe	206
Figure 4.60	The proposed structures of inclusion complex and surface binding between $\beta\text{CD-IL}$ and Phe	207
Figure 4.61	Absorption spectra of (a) βCD ; (b) Phe; (c) inclusion complex with $[\text{Phe}]$: 0.01 mM and $[\beta\text{-CD}]$: 0.0032 M; at pH 7, T = 298 K	209

Figure 4.62	Absorption spectra of (a) β CD-IL; (b) Phe; (c) inclusion complex with [Phe]: 0.01 mM and [β CD-IL]: 0.06 mM; at pH 7, T = 298 K	209
Figure 4.63	Absorption spectra of Phe with various concentration of β CD at pH 7, T = 298 K. From lines (a) to (g): 0 M; 0.001 M; 0.003 M; 0.005 M; 0.006 M; 0.008 and 0.010 M	211
Figure 4.64	Absorption spectra of Phe with various concentration of β CD-IL at pH 7, T = 298 K. From lines (a) to (e): 0 M; 0.01 mM; 0.03 mM; 0.04 mM and 0.05mM	211
Figure 4.65	Reciprocal plot for $1/[A-A_0]$ against $1/[\beta\text{-CD}]$ of the β CD-Phe inclusion complex	213
Figure 4.66	Reciprocal plot for $1/[A-A_0]$ against $1/[\beta\text{CD-IL}]$ of the β CDIL-Phe inclusion complex	213
Figure 4.67	3D view of (a) β -cyclodextrin; (b) Phe; and (c) inclusion complex of β CD: Phe 1:1 model	217
Figure 4.68	3D view of (a) β CD-IL; (b) Phe; (c) inclusion complex of β CD-IL: Phe 1:1 model; and (d) surface binding of Phe near the IL group	218
Figure 4.69	Schematic presentation of the truncated cone shape of the β CD and Phe with bond distance	219
Figure 5.1	Cyclic voltammograms of (a) bare GCE (b) Fe_3O_4 , (c) $\text{poly}(\beta\text{CD})@\text{Fe}_3\text{O}_4$ and (d) $\text{poly}(\beta\text{CD-IL})@\text{Fe}_3\text{O}_4$ recorded in the aqueous solution of 5 mM $[\text{Fe}(\text{CN})_6]^{3-/4-}$ solution containing 0.1 M phosphate buffer solution (PBS) (1:1) at a scan rate of 100 mV s^{-1}	223
Figure 5.2	The absorption spectra of RhB (a) before and after adsorption, (b): Fe_3O_4 , (c) $\text{poly}(\beta\text{CD})@\text{Fe}_3\text{O}_4$ and (d) $\text{poly}(\beta\text{CD-IL})@\text{Fe}_3\text{O}_4$	224

LIST OF ABBREVIATIONS

[C4min] PF ₆	1-butyl-3-methylimidazolium hexafluorophosphate
[Fe(CN) ₆] ^{3-/4-}	Potassium ferricyanide
[Hmim]BF ₄	1-hexyl-3-methylimidazolium tetrafluoroborate
Ace	Acenaphthalene
ACN	Acetonitrile
APTES	(3-aminopropyl)triethoxysilane
BaA	Benzo(a) anthracene
BaP	Benzo(a) pyrene
BBD	Box-Behnken design
BET	Brunauer Emmelt Teller
BGE	Background electrolyte
BMIMBF ₄	1-butyl-3-methyl-imidazolium tetrafluoroborate
C	Carbon
Cd(II)	Cadmium (II)
CE	Capillary electrophoresis
CPE	Cloud point extraction
Cr ⁶⁺	Chromium (VI) ion
DNA	Deoxyribonucleic acid
DSC	Differential scanning calorimetry
EA	Elemental analysis
EC	European Community
FAAS	Flame atomic absorption spectroscopy
Fe ₃ O ₄	Iron(II, III) oxide
FF-DLPME	Ferrofluid-based dispersive liquid phase microextraction

Fla	Fluoranthene
Flu	Fluorene
FSQD	Food Safety and Quality Division
FTIR	Fourier transform infrared
GC- μ ECD	Gas chromatography-micro electron capture detector
GCE	Glass carbon electrode
GC-FID	Gas chromatography- flame ionization detector
GC-MS	Gas chromatography–mass spectrometry
H	Hydrogen
H ₃ PO ₄	Phosphoric acid
HDI	Hexamethylene diisocyanate
HPLC-FLD	High-performance liquid chromatography-fluorescence detector
HPLC-UV	High-performance liquid chromatography-ultraviolet detector
HP- β -CD	(2-hydroxypropyl)- β -cyclodextrin
ICH	International Conference on Harmonization
IL	Ionic liquid
LLE	Liquid-liquid extraction
LOD	Limit of detection
LOQ	Limit of quantification
LPME	Liquid-phase microextraction
Magnetic μ -SPE	Magnetic micro-solid phase extraction
ME	Microextraction
Me- β -CD	Methylated- β -cyclodextrin
MeOH	Methanol

MgAl-LDH	Magnesium–aluminum layered double hydroxide
Mn(II)/Mn(VII)	Manganese (II) and Manganese (VII)
MNPs	Magnetic nanoparticles
MSPE	Magnetic solid phase extraction
N	Nitrogen
NaCl	Sodium chloride
NaH ₂ PO ₄	Monosodium phosphate
NaOAc	Sodium acetate
NaOH	Sodium hydroxide
Nap	Naphthalene
ND/ n.d	Not detected
NH ₄ Cl	Ammonium chloride
NMR	Nuclear magnetic resonance
NTf ₂	Bis(trifluoromethylsulfonyl)amide
OVAT	One-variable-at-a-time
PAHs	Polycyclic aromatic hydrocarbons
PAN	Polyacrylonitrile
PBS	Phosphate buffer solution
PF	Preconcentration factor
Phe	Phenanthrene
PM _{2.5}	Fine particulate matter
Pyr	Pyrene
RhB	Rhodamine B
RSD	Relative standard deviation
RSM	Response surface design

SCF	Scientific Community on Food
SEM	Scanning electron microscopy
SiO ₂	Silicon dioxide or silica
SPE	Solid phase extraction
SPME	Solid phase microextraction
SUPRAS	Supramolecular solvents
TDI	Toluene diisocyanate
TEM	Transmission electron microscope
TEQ	Toxic Equivalent Factor
TGA	Thermogravimetric analysis
TiO ₂	Titanium dioxide
TLC	Thin layer chromatography
TM-β-CD	Trimethylated-β-cyclodextrin
UiO-67	(University of Oslo) series-67
US EPA	United States Environmental Protection Agency
VSM	Vibrating sample magnetometer
WCA	Water contact angle
WHO	World Health Organization
XRD	X-ray powder diffraction
α-CD	Alpha-cyclodextrin
β-CD	Beta-cyclodextrin
βCD-IL	Beta-cyclodextrin functionalized ionic liquid
γ-CD	Gamma-cyclodextrin

LIST OF SYMBOLS

%	Percent
$\mu\text{g kg}^{-1}$	Microgram per kilogram
$\mu\text{g L}^{-1}$	Microgram per litre
μL	Microlitre
μm	Micrometre
A'	Absorbance of guest in the presence of host
A_0	Absorbance of guest in the absence of host
$^{\circ}\text{C}$	Degree Celsius
C_0	Centre points
D_c	Average crystalline diameter
DT	Degree of tolylation
g L^{-1}	Gram per litre
g mol^{-1}	Gram per mol
k	Number of factors
K	Apparent formation constant
kV	Kilovolt
M	Molarity
mA	Milliampere
mg L^{-1}	Milligram per litre
mM	Millimol
mmol	Millimol
mmol L^{-1}	Millimol per litre
mol L^{-1}	Mol per litre
$\text{M}\Omega$	Milliohm

N	Number of experiment
ng L^{-1}	Nanogram per litre
ng mL^{-1}	Nanogram per millimetre
nm	Nanometre
ppm	Part per million
R^2	Coefficient of determination
rpm	Rotation per minute
V	Voltage
v/v	Volume per volume
w/v	Weight per volume
K	Particle shape factor
μA	Microampere

PEMBANGUNAN POLI(β -SIKLODEKSTRIN BERFUNGSIKAN CECAIR IONIK) BERKONJUGAT NANOPARTIKEL MAGNET SEBAGAI PENJERAP UNTUK PENGEKSTRAKAN MIKRO POLISIKLIK AROMATIK HIDROKARBON DARIPADA SAMPEL MAKANAN

ABSTRAK

Pencemaran makanan merupakan isu keselamatan makanan global yang boleh menimbulkan masalah kesihatan. Analisis terhadap pencemar adalah penting untuk memastikan keselamatan pengguna dan pematuhan terhadap had peraturan. Oleh itu, pembangunan teknik penyediaan sampel yang mudah, berskala kecil, dan sensitif sentiasa menjadi pilihan yang digemari. Kajian ini bertujuan untuk membangun dan menyiasat bahan nano yang baru, iaitu poli(β CD-IL)@Fe₃O₄ dan aplikasinya dalam pengekstrakan mikro polisiklik aromatik hidrokarbon (PAHs) yang mempunyai berat molekul rendah dan tinggi yang disenaraikan sebagai bahan pencemar utama oleh Komuniti Eropah (EC) dan Agensi Perlindungan Alam Sekitar (EPA). Dalam bahagian pertama kajian, poli(β CD-IL)@Fe₃O₄ telah berjaya disintesis dan dicirikan oleh pelbagai teknik termasuk FT-IR, analisis elemen CHN, XRD, TEM, SEM, VSM, BET, TGA, DSC, potensi zeta dan ukuran kebolehasahan. Seterusnya, poli(β CD-IL)@Fe₃O₄ digunakan sebagai penjerap dalam kaedah magnetik μ -SPE bersama gas kromatografi pengesanan pengionan nyala (magnetik μ -SPE-GC-FID) untuk penentuan lima PAHs terpilih yang mempunyai berat molekul rendah dalam sampel beras. Dalam keadaan optimum, lekuk penentukuran telah menunjukkan kelinearan dalam kepekatan antara 0.1 dan 500 $\mu\text{g kg}^{-1}$ dengan pekali penentuan (R^2) di antara 0.9970 dan 0.9982 untuk kesemua analit. Had pengesanan (LODs) dalam matriks sebenar berada dalam julat 0.01-0.18 $\mu\text{g kg}^{-1}$. Nilai sisihan piawai relatif (RSD) berada pada 2.95%-5.34% (intra-hari, n=6) dan 4.37%-7.05% (antara hari, n=6). Penjerap

menunjukkan kebolehulangan yang memuaskan dalam julat 2.9% ke 9.9% dan nilai perolehan semula yang boleh diterima pada 80.4% – 112.4% untuk sampel sebenar. Kaedah optimum magnetik μ -SPE-GC-FID kemudian berjaya diaplikasikan untuk mengakses kandungan keselamatan PAHs dalam 24 jenis beras komersial yang terdapat di Malaysia. Prestasi analitikal poli(β CD-IL) $@$ Fe₃O₄ yang cemerlang dalam kaedah magnetik μ -SPE-GC-FID seterusnya menjadi dorongan untuk mengubahsuainya ke bentuk bendalir ferro dalam membangunkan teknik FF-DLPME di bahagian kedua kajian ini. Bendalir ferro ini telah digunakan untuk pengekstrakan mikro tujuh wakil PAHs yang mempunyai berat molekul rendah dan tinggi daripada makanan dan minuman. Dalam keadaan optimum, lekuk penentukuran telah menunjukkan kelinearan dalam kepekatan antara 0.1 dan 150 ng mL⁻¹ dalam matrik air dengan R² daripada 0.9970 ke 0.9982 untuk kesemua analit. LODs kaedah adalah dalam julat 0.02 dan 0.07 ng mL⁻¹. RSD, % untuk intra-hari dan antara hari berada dalam julat 1.80%-7.56% dan 2.97%-8.23% dengan nilai kebolehulangan di antara 1.72% dan 5.90%. Manakala, nilai perolehan semula adalah pada 84%-110% untuk sampel sebenar. Parameter yang sama turut disahkan dalam matrik beras dan minuman teh. Kaedah optimum FF-DLPME-GC-FID akhirnya diaplikasikan untuk menilai kandungan keselamatan PAHs dalam pelbagai jenis makanan dan minuman komersial di Malaysia. Perbandingan antara kedua-dua teknik pengekstratan mikro yang dibangunkan juga telah dibentang. Akhir sekali, mekanisma penjerapan berdasarkan kajian kompleks telah dijalankan untuk menyiasat kehadiran interaksi supramolecular host-guest yang menyumbang kepada prestasi cemerlang pengekstrakan mikro bagi kedua-dua teknik. Pembentukan kompleks pepejal telah berjaya dipantau oleh pengukuran teknik FTIR, TGA, DSC, 1D 1H NMR dan 2D NOESY NMR, manakala kompleks cecair berjaya dipantau oleh pengukuran spektroskopi UV-vis. Keputusan

menunjukkan bahwa Phenanthrene membentuk nisbah stoikiometri 1:1. Skema daripada proses pembentukan kompleks yang dicadangkan oleh kajian doking molekul menyerupai keputusan eksperimen.

**DEVELOPMENT OF POLY(β -CYCLODEXTRIN FUNCTIONALIZED
IONIC LIQUID) CONJUGATED MAGNETIC NANOPARTICLES AS AN
ADSORBENT FOR MICROEXTRACTION OF POLYCYCLIC AROMATIC
HYDROCARBONS FROM FOOD SAMPLES**

ABSTRACT

Food contamination is a global food safety issue which pose a health concern. Analysis of food contaminants is essential to ensure consumer safety and compliance with regulatory limits. Thus, development of simple, miniaturize, and sensitive sample preparation techniques are always a choice of interest. This study aims to develop and investigate new nanomaterial, namely poly(β CD-IL) $@$ Fe₃O₄ and their applications in the microextraction of low and high molecular weight polycyclic aromatic hydrocarbons (PAHs) that have been listed as priority pollutants by European Community (EC) and Environmental Protection Agency (EPA). In the first part of study, poly(β CD-IL) $@$ Fe₃O₄ was successfully synthesized and characterized by various techniques including FT-IR, CHN elemental analysis, XRD, TEM, SEM, VSM, BET, TGA, DSC, zeta potential and wettability measurement. Thereafter, poly(β CD-IL) $@$ Fe₃O₄ was applied in magnetic μ -SPE technique as an adsorbent coupled with gas chromatographic-flame ionization detection (magnetic μ SPE-GC-FID) for the determination of five selected low molecular weight PAHs in rice samples. Under optimized conditions, the calibration curves were linear for the concentration ranging between 0.1 and 500 μ g kg⁻¹ with coefficient of determination (R^2) from 0.9970 to 0.9982 for all analytes. Detection limits (LODs) ranged at 0.01–0.18 μ g kg⁻¹ in real matrix. The RSD values ranged at 2.95%–5.34% (intra-day, n=6) and 4.37%–7.05% (inter-day, n=6). The sorbent showed satisfactory reproducibility in 2.9% to 9.9% range and acceptable recovery values at 80.4%–112.4% for the real samples. The

optimized magnetic μ -SPE-GC-FID method was then successfully applied to assess the content safety of selected PAHs for 24 kinds of commercial rice available in Malaysia. The excellent analytical performance of poly(β CD-IL) $@\text{Fe}_3\text{O}_4$ in magnetic μ -SPE technique further became a driving force to modify it into ferrofluid, turning out with a ferrofluid-based dispersive liquid phase microextraction (FF-DLPME) technique, which was covered in the second part of this study. The ferrofluid was applied for the microextraction of seven representative PAHs including low and high molecular weight PAHs from food and beverages. Under optimized conditions, the calibration curves were found to be linear in water matrix from a range of 0.1-150 ng mL⁻¹ with R² between 0.9944 and 0.9986. The LODs of the proposed method were between 0.02 and 0.07 ng mL⁻¹. The intra and inter-day precision (RSD, %) were in the range of 1.80%-7.56% and 2.97%-8.23% with sorbent reproducibility between 1.72% and 5.90% and acceptable recovery values at 84% -110% for real samples. Similar validation parameters also have been conducted in rice and tea beverage matrices. The optimized FF-DLPME-GC-FID method was finally applied to evaluate the content safety of studied PAHs in a variety of commercial foods and beverages in Malaysia. Comparison between both developed microextraction techniques is presented. Lastly, adsorption mechanism based on inclusion complex study was conducted to investigate the presence of supramolecular host-guest interaction that contributes to the excellent extraction performance for both developed microextraction techniques. The formation of solid kneaded inclusion complex was successfully monitored by FTIR spectroscopy, TGA, DSC, 1D ¹H NMR and 2D NOESY NMR measurement, whereas liquid inclusion complex was monitored by UV-vis spectroscopy. Results revealed that Phenanthrene formed a 1:1 stoichiometry ratio. A schematic representation of the energetically

favorable inclusion process is proposed by molecular docking studies which is in good agreement with the experimental results.

CHAPTER 1

INTRODUCTION

1.1 General background

In recent years, there has been a growing concern among the general public over the issue of food contamination by toxic compounds, particularly polycyclic aromatic hydrocarbons (PAHs). Generally, PAHs tend to accumulate in food products such as dairy, vegetables, fruits, oils, rice, cereals, grilled meat, smoked food, coffee, and tea (Bansal & Kim, 2015; Boon et al., 2019; Chung et al., 2011; Escarrone et al., 2014; Farhadian et al., 2010; Iwegbue et al., 2016; Jimenez et al., 2014; Lochan et al., 2016; Pincemaille et al., 2014; Plaza-Bolaños et al., 2010; Smoker et al., 2010; Yun et al., 2017; Zachara et al., 2018; Zelinkova & Wenzl, 2015; Zheng et al., 2016) due to their hydrophobic and lipophilic characteristics (Pensado et al., 2005). Many works have identified food as major contributor to human direct exposure to PAHs and therefore, their presence in food is a matter of concern.

PAHs are compounds that contain two or more fused benzene rings in a linear, angular or cluster arrangement (Shi et al., 2016). They are formed from the incomplete combustion (engine exhaust, industrial outlet, crude oil) or pyrolysis of organic matter (Chen & Chen, 2001; Zhao et al., 2011) and are widespread in the environment as organic pollutants (Jiao et al., 2007; Xu et al., 2014). Sixteen priority PAHs have been listed as persistent organic pollutants (POPs) by the U.S. Environmental Protection Agency (US EPA) due to their substantial toxicity and possible carcinogenic properties (Aguinaga et al., 2007; Fei et al., 2011; Jimenez et al., 2014). Furthermore, PAHs are

also highly resistant to natural degradation due to their stable molecular structures (Lau et al., 2014).

The occurrence of PAHs in food can be ascribed to diverse pathways that include both natural (as environmental) and synthetic sources (e.g. cooking practices and industrial food processing). Upon ingestion, PAHs will activate the mammalian cells to produce diolepoxides that will react with the DNA in tissue cells to cause mutation (Bansal & Kim, 2015).

Numerous efforts have been directed to address how precisely and accurately one can qualify and quantify the level of PAHs present in food products and this is non-trivial since food is typically non-homogenous and complex that make it hard to isolate and determine the analyte of interest.

“Direct and shoot” concepts using chromatography or spectroscopy method may experience some sensitivity issues which can lead to poor analysis result besides increasing the instrument maintenance. Subsequently, by considering the food matrix effects, many analytical methods that have been developed for monitoring and determining the food contaminations generally involve a pre-treatment step prior to instrumental analyses. Sample pre-treatment or sample preparation is regarded to be an important step in a chemical analysis as it aims to extract, pre-concentrate, and clean-up from interference apart from the advances in analytical instrumentation for analyte separation and detection. Sample preparations also improve the analysis results by enhancing the sensitivity, precision and instrument detection limits which could not be achieved by direct determination at a very low concentration. Thus, a good sample preparation can be economically valuable as well as analytically important.

1.2 Problem Statements

The level of PAHs in food have been regulated by the World Health Organization (WHO) due to their toxicity to human (Registry, 2008). For instance, 4 high molecular weight PAHs namely PAH4 (benzo(a)pyrene, benz(a)anthracene, benzo(b)fluoranthene and chrysene) have been selected as food markers by the Commission Regulation (EU) No 835/2011 with their maximum limits between 1 and 30 $\mu\text{g kg}^{-1}$ (Food Safety Authority of Ireland, 2015). However, there's still a need for reliable data on other PAHs, especially those with low molecular weight as they are more commonly found compared to high molecular weight PAHs that listed in food legislation (Escarrone et al., 2014; Matin et al., 2014; Plaza-Bolaños et al., 2010). Indeed, the Scientific Committee on Food (SCF) has urged the collection of data based on other types of PAHs in assessing food contamination and to monitor the changes of PAHs profile in food (Zelinkova & Wenzl, 2015).

By narrowing the scope of PAHs investigation in Malaysia, surprisingly, number of study regarding to the PAHs determination in food and beverage samples are far less compared to environmental samples. This reveals that inadequate attention has been paid, likely due to the absence of legislation concerning the safety levels of food PAHs in our country. Since PAHs can accumulate in the human body through food consumption, their analysis is essential to ensure the consumers' safety.

Different sample preparation techniques and separation methods have been developed and reported for PAHs determination. Among the sample preparations techniques, sorbent-phase based extraction technique stands out the most popular one. Various types of adsorbents have been designed to satisfy the applications. However, most of these adsorbents are tuned with the focus on their affinity for target analytes,

but with little consideration on their compatibility towards the sample matrices. Furthermore, PAHs usually exhibit low solubility and bioavailability (Ren et al., 2015), which limits their removal or extraction from the contaminated food.

Herein, supramolecular cyclodextrins (CDs) appear to be particularly promising agent through host-guest interaction as reported in previous works (Choi et al., 2017; Topuz & Uyar, 2017b, 2017a). This could be contributed by the merit of CDs which are able to reduce the toxicity, enhance the solubility and catalyse the degradation of contaminants (Bardi et al., 2000; Boving & Brusseau, 2000; Kamiya et al., 2001; Manolikar & Sawant, 2003). Moreover, CDs prevail other adsorbents due to their biocompatibility, non-toxic and environmentally friendly properties (Choi et al., 2017).

Recently, microextraction techniques have been developed as an alternative method for the determination of trace level compounds and are gaining much interests since these techniques greatly reduce the volume of organic solvent, sorbent dosage, and extraction times coupled with inexpensive instruments. Nonetheless, there is still a need to develop microextraction techniques that comply with the principles of green chemistry.

In the attempt to comprehensively address the above-mentioned issues, this study is systematically conducted.

We hope the findings in this study could be a preliminary benchmark or added value to the existing data for the establishment of the maximum permissible limits of food PAHs to Food Safety and Quality Division (FSQD), Ministry of Health Malaysia. In addition, we anticipate that the study outcomes provide insight and awareness into the rational diet suggestions to maintain or improve public health.

1.3 Scope of research

This study involves the synthesis of a nanocomposite, namely poly(β CD-IL) conjugated magnetic nanoparticles which combines the merits of polymeric β -CD, IL, and magnetic nanoparticles. It is important to highlight the rationality for such a design and fabrication of the nanocomposite since different organic moieties possess their own unique properties that contribute to the extraction efficacy. For this, β -CD is chosen instead of α - and γ - cyclodextrin due to its low cost, stability and is commercially available. Besides, it is well known that β -CD are guest friendly that is able to interact with various kinds of organic molecules by forming inclusion complex. In addition, the odd number of glucose rings present in its structure decreases the symmetry of the cavity, hence, increasing the resolving power of β -CD. This unique property has received great attention and is fully exploited by researchers in the field of separation sciences. On the other hand, IL is employed as modifier to increase the active sites of the nanocomposite. Due to the presence of double bonds, it can be used to extract the analytes through π to π adsorption mechanism. Herein, 1-vinylimidazole was selected in the modification process to give rise to 1-vinylimidazolium- β -CD as the unique functional monomer. However, the chemically modified cyclodextrins are soluble, which limit their applications in water, therefore, conversion of modified CD to polymeric materials is of great values. To attain this property, cross-linker agent (toluene-2,4-diisocyanate) was utilized to produce water insoluble IL modified cyclodextrin polymers. This polymer host networks are further grafted on the surface of magnetic nanoparticles in order to promote the developed sample preparation techniques.

In short, the application of β -CD and IL are to provide multiple binding sites to the nanocomposite while the employment of toluene-2,4-diisocyanate is to

polymerize the soluble entities. Meanwhile, magnetic nanoparticles are decorated to make the nanocomposites separate easily by means of external magnetic field and to improve the adsorption capacity by its large specific surface area. The synthesized nanocomposite is expected to exhibit few unique properties such as high surface area, high supramolecular recognition capability, superparamagnetism and large delocalized π -electron system.

The successful synthesis of this nanocomposite was confirmed by various characterization techniques such as Fourier transform infrared (FTIR), elemental analysis, Brunauer-Emmett-Teller (BET), vibrating sample magnetometer (VSM), scanning electron microscopy (SEM), transmission electron microscopy (TEM), x-ray powder diffraction (XRD), thermogravimetric analysis (TGA), differential scanning calorimetry (DSC), zeta potential and wettability analysis. Thereafter, it was being applied in magnetic μ -SPE for the determination of selected low molecular weight PAHs from rice samples coupled with GC-FID. The excellent analytical performance of the developed nanocomposite in magnetic μ -SPE technique was encouraging and further became a driven force to modify the nanocomposite into ferrofluid turning out with FF-DLPME technique. Due to the merits of ferrofluid, it was successfully applied for the analysis of selected low and high molecular weight PAHs in various food and beverage samples. Subsequently, the extraction performances of both developed magnetic μ -SPE and FF-DLPME methods were then compared. Investigation on the adsorption mechanism by means of inclusion complex study was also conducted. A schematic representation of the energetically favorable inclusion process is proposed by molecular docking studies using PatchDock server.

1.4 Research Objectives

The objectives of this work are summarized as follows:

- (i) To synthesize and characterize Ts_2O , $\beta\text{CD-OTS}$, $\beta\text{CD-Vinyl-OTS}$, Fe_3O_4 , $\text{poly}(\beta\text{CD})@\text{Fe}_3\text{O}_4$, and $\text{poly}(\beta\text{CD-IL})@\text{Fe}_3\text{O}_4$
- (ii) To develop, optimize, and validate $\text{poly}(\beta\text{CD-IL})@\text{Fe}_3\text{O}_4$ based magnetic $\mu\text{-SPE}$ techniques coupled with GC-FID analysis for the determination of low molecular weight PAHs in rice samples
- (iii) To develop, optimize, and validate $\text{poly}(\beta\text{CD-IL})@\text{Fe}_3\text{O}_4$ based FF-DLPME techniques coupled with GC-FID analysis for the determination of low and high molecular weight PAHs in food and beverage samples
- (iv) To compare the analytical performance of $\text{poly}(\beta\text{CD-IL})@\text{Fe}_3\text{O}_4$ based magnetic $\mu\text{-SPE}$ and FF-DLPME techniques
- (v) To investigate the adsorption mechanism of Phenanthrene via inclusion complex study between the native $\beta\text{-CD}$ and ionic liquid modified $\beta\text{-CD}$

1.5 Organization of thesis

The present thesis is organized into five chapters. Chapter 1 outlines a brief introduction on the research background, problem statement, scope of research, research objective, and a structural organization of the whole thesis. A review of related literature is summarized in Chapter 2. Chapter 3 discusses the experimental procedures for the whole study and subdivided into five parts. Part one to part three describe about the synthesis methods and characterization techniques of adsorbents whereas part four reports the method development, validation and applications of the adsorbents in magnetic μ -SPE and FF-DLPME techniques, respectively. While investigation on the adsorption mechanism by means of inclusion complex and molecular docking are presented in final part. Chapter 4 consists of six parts that discuss the findings and outcomes of the study accordingly. The overall conclusions and further recommendations are presented in Chapter 5.

CHAPTER 2

LITERATURE REVIEW

2.1 Magnetic nanoparticles (MNPs)

2.1.1 Synthesis of MNPs

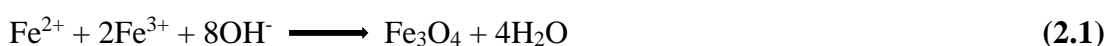
Researches and development of nano-based materials have gained a lot of attractions within the scientific community. The focus is primarily on designing particles that have uniform shape, arrangement, and nano-meter size. For this, metallic and metal oxides NPs have been widely exploited in the field of analytical chemistry due to their tuneable properties which are able to offer promising applications in terms of sensitivity, selectivity and reliability.

Magnetic nanoparticles (MNPs) are a type of metal oxides NPs, which can be handled by using an external magnetic field. Their large surface areas to volume ratio, high dispersibility (Amirhassan et al., 2015), quantum size effects, supraparamagnetic behaviour, and easiness of surface modification allow them to be used in a wide range of applications, including magnetic drug target (Pecina, 1978), nano-sorbent in environmental engineering (Awwad & Salem, 2013), magnetic resonance imaging (Anbarasu & Balamurugan, 2014; Yugandhar et al., 2013), biomedicine (Barrera et al., 2009), and magnetic sensing (Jun-Hua et al., 2007)

Maghemite (Fe_2O_3) and magnetite Fe_3O_4 are the most common iron oxides used to synthesize MNPs due to their biological compatibility, high magnetic moment, and easy to prepare. For this, ferrite oxide magnetite (Fe_3O_4) that possess large surface

area with nano-size dimension, excellent sorption capability, and strong response under an applied external magnetic field have been the focus of many research works.

Fe₃O₄ nanoparticles can be prepared using different ways such as laser ablation, mechanical grinding, chemical precipitation, high temperature decomposition of organic precursor, and microemulsion (Sun et al., 2004). The most employed method is chemical precipitation due to their low cost and simplicity preparation. This method involves mixing ferrous (II) and ferric (III) ions in molar ratio of 1:2 in highly basic solution at elevated or room temperature (Cabrera et al., 2008). **Equation 2.1** explains the synthesis route of magnetite nanoparticles through co-precipitation process.



2.1.2 Surface modification of MNPs

Basically, MNPs tend to agglomerate due to their high surface energies resulting from their large surface area and volume ratio. Besides, unmodified MNPs also easily undergo oxidation which can cause the loss in their magnetic and dispersibility property, as well as difficulty to control their shape, size, and stability.

To address this problem, surface modification has been introduced to the design and fabrication of Fe₃O₄ with specific functionality and activity. Surface modifications are not only able to improve the stability of MNPs and their dispersion, but also enhance their compatibility in solid, liquid or biological matrices. In addition, surface modification also provides channel for further immobilizing, grafting and coating of additional organic or inorganic moiety (Rós & Zougagh, 2016). Surface modification generally involves three steps, including the synthesis of core (magnetite or maghemite), the coating of the magnetic core and the modification of the resultant

core-shell structure. **Figure 2.1** shows different types of shells and functional groups or final coatings that can be anchored/coated onto the MNPs surfaces.

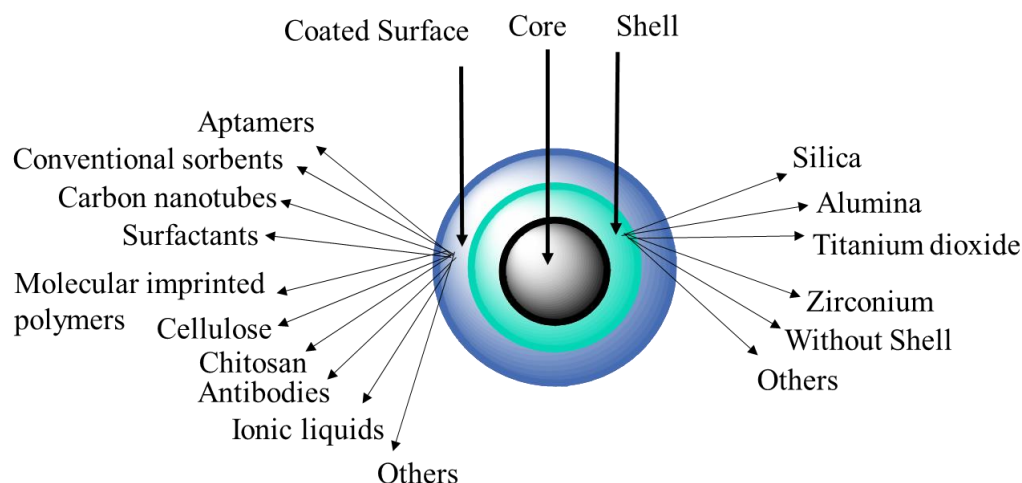


Figure 2.1: Structure of the core, shell of various composition, and the coating with different functional groups (R ós & Zougagh, 2016)

2.1.3 MNPs in analytical chemistry

In the context of analytical chemistry, modified MNPs have been widely applied in sample preparation, analyte separation and electrochemical sensing.

2.1.3(a) Modified MNPs in sample preparation

Lately, magnetic solid phase extraction (MSPE) has become a favorable technique among researchers because it simplifies the overall extraction procedures. Instead of packing the sorbent into SPE cartridge, the sorbent are being dispersed in the sample solution. This greatly facilitate the extraction rate due to better surface area of contact between analyte and sorbent. Furthermore, MSPE also avoid laborious steps such as filtration or centrifugation as the sorbents can be easily collected by using an external magnet. The applications of modified MNPs in MSPE are tabulated in **Table 2.1**.

Table 2.1: Selected examples of modified MNPs used in MSPE

Core/Shell	Functional group/ Coating	Analyte	Sample	Reference
Fe ₃ O ₄ /SiO ₂	2-mercapto-4-methyl-5-thiazoleacetic acid bonding Au (MMTA-Au)	polycyclic aromatic hydrocarbons	river water and rainwater	(Xiupei et al., 2019)
Fe ₃ O ₄	ferric sulfate hexahydrate and ferric chloride hexahydrate	polycyclic aromatic hydrocarbons	produced water from wells	(De Barros Caetano et al., 2019)
Fe ₃ O ₄	-	rivastigmine	bulk and capsules	(Mohamed et al., 2019)
Fe ₃ O ₄	curcumin loaded magnetic graphene oxide	parabens	toothpaste and mouthwash samples	(Razavi & Es'haghi, 2019)
Fe ₃ O ₄ @APTES	silicone-ethylene-oxide copolymer (DC193C)	parabens	river water, seawater and lake water	(Marinah et al., 2019)
Fe ₃ O ₄	polydopamine	human genomic DNA	human whole blood	(Min et al., 2019)
Fe ₃ O ₄ @APTES	polyamidoamine dendrimer	tetrabromo- bisphenol A and 4-nonylphenol	environmental water	(Yalin et al., 2019)
Fe ₃ O ₄ /SiO ₂	mesoporous silica nanoparticles (MCM-41)	biogenic amines	traditional dairy product	(Molaei et al., 2019)
Fe ₃ O ₄	reduced graphene oxide (rGO)	phenolic compounds	oilseeds	(Lang et al., 2019)

2.1.3(b) Modified MNPs in separation science

Modified MNPs have also been studied in improving the resolution of electrophoretic and chromatographic separations. MNPs are typically being modified into stationary or pseudostationary phases which can achieve better outcomes compared to traditional phases. This can be attributed to their high adsorption capacity, longer lifetime and excellent surface chemistry. **Table 2.2** presents the application of MNPs in analyte separation.

Table 2.2: Selected examples of modified MNPs used in separation science

Material	Functional group/ Coating	Detection	Analyte	Reference
Molecularly imprinted magnetic nanoparticles	methacrylic acid and ethylene glycol dimethacrylate on 3-(methacryloyloxy)propyltrimethoxysilane	CE	racemic ofloxacin	(Qu et al., 2010)
Carboxyl functionalized magnetic cores	UiO-67 metal-organic frameworks	HPLC	phenol	(Weiwei et al., 2015)
Magnetic nanoparticles	β -cyclodextrin and mono-6-deoxy-6-(1-methylimidazolium)- β -cyclodextrin tosylate	CE	dansylated amino acids	(Xuan et al., 2019)

2.1.3(c) Modified MNPs in electrochemical sensing

Another important application of MNPs is in electrochemistry to enhance the electrochemical detection of analytes. Low electronic transmission resistance, large surface area, and ability to detect biological and chemical compounds are among the advantages offered by MNPs-modified electrodes. Moreover, the application of MNPs in the electrode composite also helps to reduce the surface deterioration, to increase the electrocatalytic activity and to simplify the immobilization process of functional molecules. **Table 2.3** summarizes some of the applications of MNPs in electrochemical sensors.

Table 2.3: Selected examples of modified MNPs used in electrochemical sensor

Magnetic Material	Detection	Analyte	Reference
Enzyme modified magnetic nanoparticles	amperometric	glucose	(Sheng et al., 2012)
Ferromagnetic carbon encapsulated iron nanoparticles	linear scan voltammetry and electrochemical quartz microbalance	haemoglobin	(Matysiak et al., 2015)
Chitosan coated Fe ₃ O ₄ magnetic nanoparticle	amperometric	morphine	(Dehdashtian et al., 2016)
Magnetic nanoparticles decorated with monoclonal antibodies	linear scan voltammetry	transferrin	(Matysiak et al., 2017)
Magnetic nanoparticle decorated graphene	cyclic voltammetry	hydrogen peroxide	(Waifalkar et al., 2018)
Silica embedded magnetic nanoparticles	amperometric	nitrite	(Ispas et al., 2018)
Zinc iron oxide modified screen printed electrode	amperometric	sertraline	(Tajik et al., 2019)
Haemoglobin immobilized with magnetically molecularly imprinted nanoparticles	cyclic voltammetry, differential pulse voltammetry and electrochemical impedance spectroscopy	3-chloro-1, 2-propandiol	(Yuan et al., 2019)

2.2 Cyclodextrin

2.2.1 Properties of cyclodextrin

Supramolecular chemistry is a discipline in chemistry that has recently received a great deal of attention. It provides a thorough understanding that there are no covalent bonds between the interacting species as most interactions involve host-guests interaction. Among various hosts, cyclodextrins (CDs) have been recognised as the most popular host as it can fit various types of guest molecules with suitable polarity and dimensions in their cavities (Ain et al., 2015; Malefetse et al., 2009; Raoov et al., 2013, 2014; Sambasevam et al., 2013; Sharifah et al., 2011; Singh & Bharti, 2010; Surikumaran et al., 2014). Example of guests molecules include straight or branched chain of aliphatics, aldehydes, ketones, alcohols, ionic liquid, organic acids or fatty acids, and polar compounds such as amines, oxyacids, and halogens (Charoensakdi et al., 2007). Due to their versatile nature, CDs are readily modified or functionalized in order to improve their complexation capability (Song & Purdy, 1992), leading to remarkable advances in analytical applications.

CDs belong to the series of macro cyclic torus-shaped oligosaccharides which are composed of α (6), β (7), and γ (8) -CD (**Figure 2.2**) connected by α -1,4 glucopyranose units) (**Figure 2.3**). Due to the presence of carbon and hydrogen atoms, they have a hydrophobic interior cavity (**Figure 2.4**) and this feature enables them to host various hydrophobic compounds in their cavities without having to form chemical bonds (**Figure 2.5**). Whereas the presence of hydroxyl groups on the outer part of the torus surface cause the exterior to be hydrophilic. β -CD is less soluble in water compared to α -CD and γ -CD. This is because in α -cyclodextrins, the hydrogen belt is incomplete since one of the glucopyranose unit is distorted and only four out of six possible H-bonds can be formed. Meanwhile, γ -CDs have a non-coplanar and flexible

structure causing it to be the most soluble among the three CDs. Several characteristics of the three different CDs are summarize in **Table 2.4**.

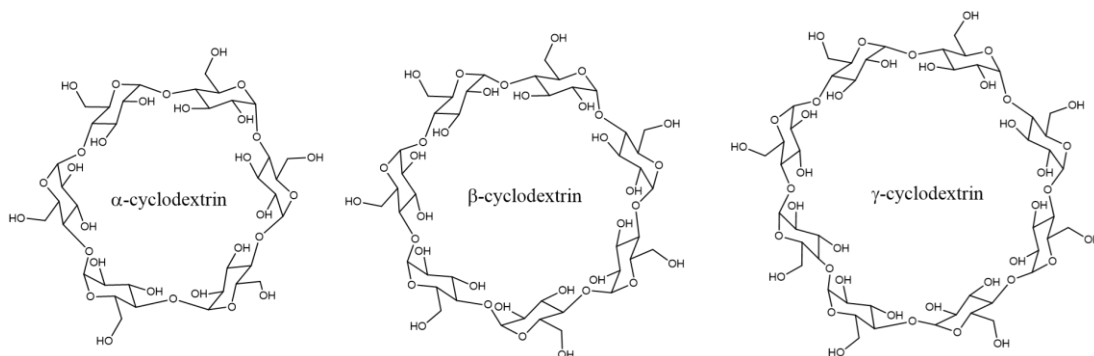


Figure 2.2: Chemical structure of α -CDs, β -CDs and γ -CDs

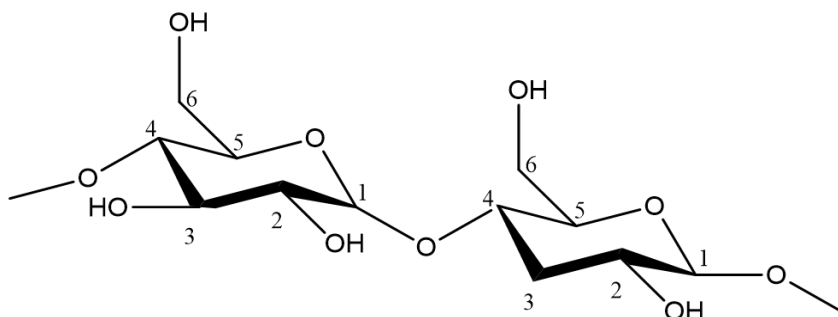


Figure 2.3: α -1,4 glucopyranose units linkages and the numbering system in a CD molecule

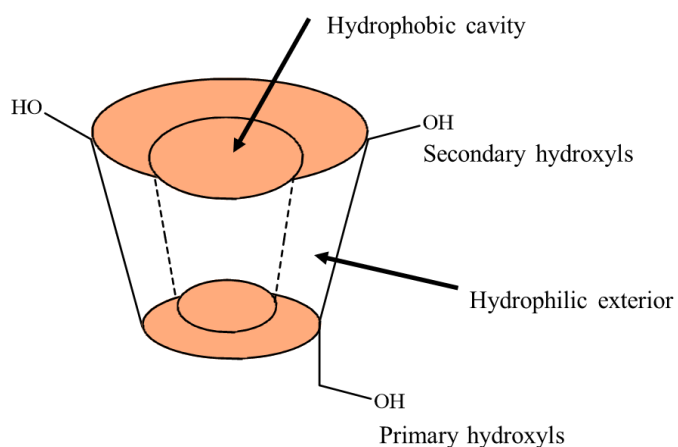


Figure 2.4: Hydrophobic cavity and hydrophilic exterior of a CD molecule

Table 2.4: Characteristics of α , β , γ - cyclodextrins (Szejtli, 1988)

Cyclodextrin	Molecular weight (g mol ⁻¹)	Solubility in water at 25°C (g/100 mL)	Volume of cavity (Å ³)	Cavity diameter (Å)	Outer diameter (Å)	Torous height (Å)
α	972	14.5	174	4.7-5.3	14.6	7.9
β	1135	1.85	262	6.0-6.5	15.4	7.9
γ	1297	23.2	427	7.5-8.3	17.5	7.9

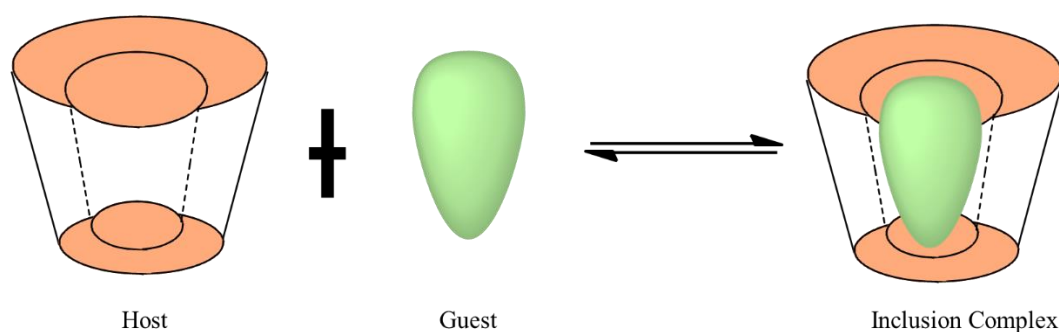


Figure 2.5: Schematic illustration of the association of free host (cyclodextrin) and guest molecules to form inclusion complex

2.2.2 Toxicological considerations

Generally, natural CDs and their hydrophilic derivatives can hardly permeate through biological membranes which are lipophilic such as the eye cornea (Del Valle, 2004). Besides, toxicity tests have shown that orally ingested CDs is essentially harmless because absorption through gastrointestinal tract is unlikely to occur (Irie & Uekama, 1997).

2.2.3 Cyclodextrin derivatives

2.2.3(a) Modification reactions of cyclodextrins

CDs can be chemically modified to enhance both their physical and chemical properties. They can be modified by one of these four methods (Szejtli, 1988):

- (a) Substitution of one or more H-atom of the primary and/or secondary hydroxyls
- (b) Substitution of one or more primary and/ or secondary hydroxyls
- (c) Elimination of the hydrogen atom from the C5-CH₂OH group
- (d) Splitting one or more C2 and C3 bonds by periodate oxidation

There are two important factors that need to be taken into consideration when modifying cyclodextrin: the nucleophilicity of the hydroxyl groups at the C2-, C3- and C6 carbon and the tendency of cyclodextrins to form complexes with the reagent used. Among the hydroxyl groups, C6-OH is the most basic and nucleophilic, whereas, C2-OH is the most acidic and C3-OH is the most inaccessible. Consequently, electrophilic reagents will initially and primarily attack the C6-OH groups. However, more reactive groups will attack C6-OH groups and also with C2-OH and C3-OH. Apart from that, the orientation, structure, and the strength of the intermediate complex is also affected by the size of the cyclodextrin cavity (Hattori & Ikeda, 2007).

2.2.3(b) Mono-modification at the C6-position

Mono-modification of CDs involves regioselective reaction of only one targeted hydroxyl group, while per-modification involves the whole set of hydroxyl groups (Sutyagin et al., 2002). In mono-modification, C6 carbon normally will be targeted. An example modification is the reaction of β -CD with tosyl chloride in an

aqueous alkaline medium to give mono-6-tosylated β -CD. During the modification, the electrophilic tosyl chloride attacks the primary side C6-OH groups of β -CD by substituting one H-atom to form C6-tosyl- β -CD as shown in **Figure 2.6**.

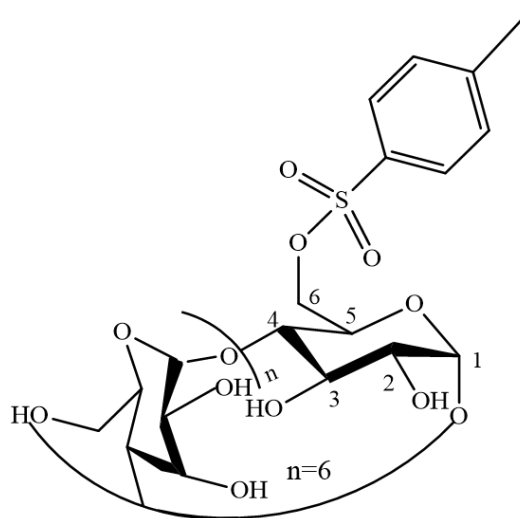


Figure 2.6: Tosylation of β -CD to form C6-tosyl- β -CD

It is interesting to point out that C6-tosyl- β -CD are important precursors for a variety of modified CDs because the tosylate group can be easily replaced by nucleophile (e.g. halogens, azides and acetates) (Mahlambi et al., 2011) that can contribute its corresponding functionality to the β -CD (Hattori & Ikeda, 2007).

2.3 Ionic liquid

Ionic liquids (ILs) are referred as liquefied organic salts at room temperature (RTIL) and are poorly coordinated. The first IL was synthesized in 1914 but its importance in the chemistry was not realised until the late 70s and 80s. Generally, ILs consists of organic cations and inorganic anions. They are designed to have a delocalized charge and one component is organic in order to prevent the formation of stable crystal lattice (Devi, 2015). ILs have been labelled as green recyclable alternatives to the conventional organic solvents and are developed to be environmentally friendly in line with the concept of sustainable chemistry (Devi, 2015; Hallett & Welton, 2011; Hernández-Fernández et al., 2010; Rahim et al., 2011; Zaijun et al., 2011). They are widely used in analytical chemistry due to their fascinating properties such as non-flammability, non-volatility, high polarity, low viscosity, and great electrochemical stability. In addition, ILs can be tuned to have desired properties by altering the combinations of cationic and anionic constituents. Because of this versatile nature, ILs are regarded as “designer solvents” and finds use as extraction solvents, catalysts, electrode modifiers (Anping et al., 2011; Mohamad et al., 2015; Mohd Rasdi et al., 2016; Sinniah et al., 2015; Yu et al., 2013), modified sorbents in sample pre-treatment and modified chiral stationary phases or additives in separation chemistry (Galán-cano et al., 2013; Huang et al., 2010; Jieping & Zhu, 2016; Jingjing et al., 2011; Miyi et al., 2016; Songqing et al., 2016; Tokaloğlu et al., 2016; Zhiming et al., 2010).

Common examples of cations and anions that have been investigated with regard to ionic liquid phase formation are shown in **Figure 2.7**.

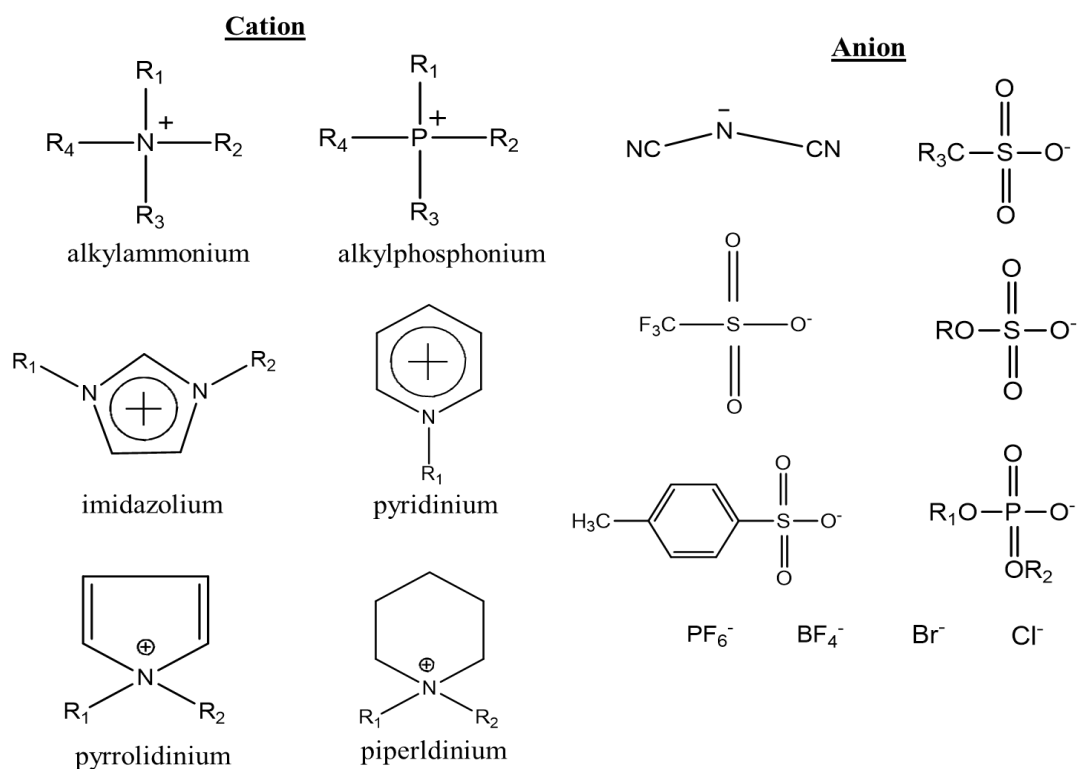


Figure 2.7: Common structures of cations and anions (Hua & Baker, 2013)

2.4 Cyclodextrins and ionic liquids-based material in analytical chemistry

Presently, the combination of CDs and ILs as advanced novel materials has received much interests as versatile tool in analytical applications. When CD-IL complexes are used, such as, in separation studies, the functional group of the ionic liquid is able to improve the extraction performance of cyclodextrin besides retaining the hydrophobic cavity of cyclodextrin molecule (Raouf et al., 2013). The behaviour of these materials are mainly dependant on the separation mechanism, which cover multiple interactions (electrostatic, hydrophobic, and $\pi - \pi$). Generally, there are two types of CD-IL complex formation processes known as functionalization and physical loading process as illustrated in **Figure 2.8**.

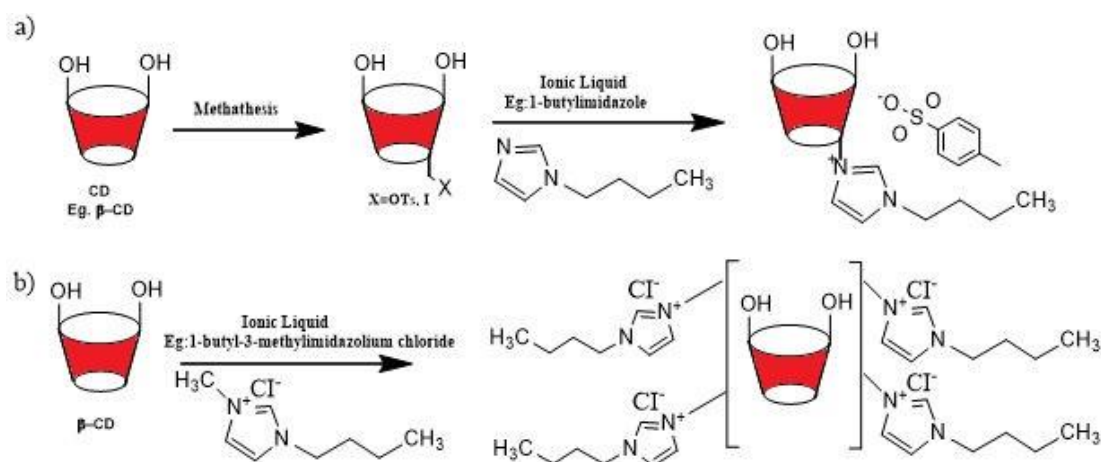


Figure 2.8: Formation of CD-IL complex through (a) functionalization process (b) physical loading process

The following part describes some applications of CD-IL materials in various separation techniques such as capillary electrophoresis (CE) (**Table 2.5**), high-performance liquid chromatography (HPLC) (**Table 2.6**), gas chromatography (GC) (**Table 2.7**), and sample preparation techniques including cloud point extraction (CPE) (**Table 2.8**), solid phase extraction (SPE) (**Table 2.9**), and microextraction (ME) (**Table 2.10**), as well as application in electrochemical sensor (**Table 2.11**). Furthermore, CD-IL modified magnetite materials also have been listed **Table 2.12**, accordingly.

Based on the reported literatures, it is interesting to point out that CD-IL based materials have combined the unique properties of cyclodextrin, ionic liquids, and magnetic nanoparticles. Therefore, they should deserve more considerations when developing excellent materials, particularly in analytical chemistry.

Table 2.5: CD-IL modified materials in CE

Type of IL	Type of CD	Analytes	Sample	BGE/Buffer	References
1-hexyl-3-methylimidazolium	α -CD	metal ions and ammonium	standard stock solution	7.5 mM lactic acid, 0.6 mM 18-crown-6, 12 mM α -CD at pH 4.0	(Qin & Li, 2004)
1-butyl-3-methylimidazolium tetrafluoroborate	β -CD	anthraquinones	chinese Herb (<i>Paedicalyx attopervensis</i> Pierre ex Pitard)	1B-3-MI-TFB [20-80 mM] and β -CD [1-6 mM]	(Qi et al., 2004)
Alkylimidazolium chlorides where alkyl= methyl, butyl, decyl, 1,2-dimethyl	β -CD	dansyl amino acid	standard solution	acid BGE at pH 6.0 and basic BGE at pH 9.6 phosphate/acetate buffer	(Ong et al., 2005)
Ethyl and phenylcholine of bis(trifluoromethylsulfonyl)imide	Di or trimethyl- β -CD	2-arylpropionic acids	anti-inflammatory drugs	acetic acid/sodium acetate (5 mM and 6 mM) at pH 5.0	(François et al., 2007)
3-methylimidazolium chloride	β -CD	dansyl amino acids	standard solution	50 mM of NaH_2PO_4 titrated with NaOH or H_3PO_4 at pH (6.5–9.6)	(Tang et al., 2007)

Table 2.5 (continued)

Alkylimidazolium chloride where alkyl= methyl, ethyl, propyl, butyl, and hexyl	β -CD	dansyl amino acid	standard solution	50 mM acetic acid in deionized water at pH 5.0 and 6.0	(Weihua et al., 2007)
N-undecenoxycarbonyl-L-leucinol bromide (L-UCLB)	2,3,6-tri-o-methyl- β -CD	ibuprofen, fenoprofen, indoprofen, suprofen, and ketoprofen	standard solution	35 mM TM- β -CD, 5 mM sodium acetate at pH 5.0	(Wang et al., 2009a)
N-undecenoxycarbonyl-L-leucinol bromide (L-UCLB)	2,3,6-tri-o-methyl- β -CD	ibuprofen, fenoprofen, indoprofen, suprofen, and ketoprofen	standard solution	5 mM NaOAc at pH 5.0 with TM- β -CD and without TM- β -CD	(Wang et al., 2009b)
6-O-2 hydroxypropyltrimethylammonium tetrafluoroborate	β -CD	bifonazole brompheniramine chlorpheniramine, liarozole pheniramine, promethazine, tropicamide, warfarin	eight racemic drugs	NaH ₂ PO ₄ (pH 2.5-5.0)	(Jia et al., 2013)
L-alanine and L-valinetert butyl ester bis (trifluoromethane) sulfonimide	Me- β -CD, HP- β -CD, and Glu- β -CD	naproxen, pranoprofen, warfarin, carprofen, ibuprofen and ketoprofen	standard solution	30 mM sodium citrate/citric acid buffer containing organic modifier (20% v/v)	(Jinjing et al., 2013)